Title:

Stable Detonation Wave Propagation in Rectangular-Cross-Section Curved Channels

Author names and affiliations:

HISAHIRO NAKAYAMA[a], TAKAHIRO MORIYA[a], JIRO KASAHARA[a], AKIKO MATSUO[b], YUYA SASAMOTO[b] AND IKKOH FUNAKI[c]

[a]*Department of Engineering Mechanics and Energy*
  University of Tsukuba
  1-1-1 Tennodai, Tsukuba, Ibaraki 305-8573, Japan
[b]*Department of Mechanical Engineering*
  Keio University
  3-14-1 Hiyoshi,Kohoku-ku, Yokohama, Kanagawa 223-8522, Japan
[c]*Institute of Space and Astronautical Science*
  Japan Aerospace Exploration Agency
  3-1-1 Yoshinodai, Chuo-ku, Sagamihara, Kanagawa 252-5210, Japan

Corresponding author:

JIRO KASAHARA

FAX/TEL: +81 29 853 5267.

E-mail address: kasahara@kz.tsukuba.ac.jp

Address: 3F109, 1-1-1 Tennodai, Tsukuba, Ibaraki 305-8573, Japan

The type of article:

Full-length article

Abstract

   The detonation propagation phenomena in curved channels were experimentally studied in order

to determine the stable propagation condition. A stoichiometric ethylene-oxygen mixture gas and

five types of rectangular-cross-section curved channels with different inner radii of curvature were

employed. The detonation waves propagating through the curved channels were visualized using a

high-speed video camera. Multi-frame short-time open-shutter photography (MSOP) was developed

in the present study to simultaneously observe the front shock shape of the detonation wave and the

trajectories of triple points on the detonation wave. The detonation wave became more stable under

the conditions of a higher filling pressure of the mixture gas and/or a larger inner radius of curvature

of the curved channel. The critical condition under which the propagation mode of the detonation

wave transitioned from unstable to stable was having an inner radius of curvature of the curved

channel (r_i) equivalent to 21 to 32 times the normal detonation cell width (λ). In the stable

propagation mode, the normal detonation velocity (D_n) increased with the distance from the inner

wall of the curved channel and approached the velocity of the planar detonation propagating through

the straight section of the curved channel (D_{str}). The smallest D_n was observed on the inner wall and

decreased with decreasing r_i/λ. The distribution of D_n on the detonation wave in the stable mode was

approximately formulated. The approximated D_n given by the formula agreed well with the

experimental results. The front shock shape of the detonation wave could be reconstructed accurately

using the formula. The local curvature of the detonation wave (κ) nondimensionalized by λ

decreased with increasing distance from the inner wall. The largest $\lambda\kappa$ was observed on the inner

wall and increased with increasing r_i/λ. D_n/D_{str} decreased with increasing $\lambda\kappa$. This

nondimensionalized D_n-κ relation was nearly independent of r_i/λ.   (300 words)

Keywords

Detonation wave; curved channel; cell width; triple point trajectory; curvature

Nomenclature

D Detonation velocity

m Exponent in Eq. (12)

p Pressure

r Distance from polar coordinate origin

t Time

T Temperature

Greek symbols

ϕ Angular difference between rotational direction and tangential direction of detonation

wave

κ Curvature of detonation wave

λ Detonation cell width

θ Angle from initial line

ω Angular velocity of detonation wave

Subscripts

0   Initial

asy   Asymptotic

CJ   Chapman-Jouguet state

i   Inner wall of curved section of flow channel

k Index of position on detonation wave

n   Normal

str   Straight section

trans   Transient

1. Introduction

A detonation wave is a self-sustained combustion wave which propagates at supersonic speed and

instantaneously generates a high pressure and temperature gas. The adiabatic compression due to the

passage of the front shock of the detonation increases the temperature of the combustible mixture

above the ignition limit, and the chemical reaction of the gas is induced. The chemical reaction

results in a heat energy release, and the expansion of the burned gas drives the front shock forward.

The detonation wave propagates self-sustainingly due to the mutual interaction between the ignition

of the combustible gas initiated by the front shock and the expansion of the burned gas.

A rotating detonation engine (RDE) is a propulsion system which generates thrust by propagating

a continuous detonation wave in an annular combustor (Braun et al. [1], Meredith et al. [2],

Kindracki et al. [3], Hishida et al. [4], Falempin and Daniau [5]). Since the RDE cycle operates with

near-constant volume combustion, RDE theoretically has a higher thermal efficiency than other

conventional propulsion systems. The RDE needs only one ignition/

deflagration-to-detonation-transition (DDT) process in principle, since the RDE utilizes a detonation

wave that propagates continuously. The increase of the thrust density of the RDE is also considered

to be easy since the propellant can be supplied continuously into the combustor chamber. For the

purpose of RDE design, it is important that the conditions for stable detonation wave propagation in

an annular combustor be well understood. However, the study of the stability of the detonation wave

propagating through a curved channel, which is a basic element of an annular combustor, is limited.

Several experimental and numerical studies on unsteady detonation waves in a curved channel (90

deg or 180 deg bend with a rectangular or circular cross-section) have been performed (Tsuboi et al.

[6], Liang et al. [7, 8], Edwards et al. [9], Thomas and Williams [10], Frolov et al. [11-14]). By

contrast, only a few studies of steady detonation waves in a curved channel have been conducted.

Kudo et al. [15] visualized the detonation waves of a stoichiometric ethylene-oxygen mixture gas

propagating through the rectangular-cross-section curved channels with constant inner/outer radii of

curvature shown in Fig. 1. They experimentally demonstrated that detonation waves could propagate

steadily and stably through the curved channels. Sasamoto et al. [16] also showed the existence of a

detonation wave propagating stably in a curved channel by two-dimensional numerical simulation.

Kudo et al. [15] observed the propagation modes of the detonation waves in the curved channels.

Using the normal detonation velocity on the inner wall of a curved channel ($D_{n,i}$) and CJ detonation

velocity (D_{CJ}), they categorized the propagation modes into three types: the stable mode ($D_{n,i}/D_{CJ} \geq$

0.8), the critical mode ($D_{n,i}/D_{CJ} \geq 0.6$), and the unstable mode ($D_{n,i}/D_{CJ} < 0.6$). They also showed that

the critical condition under which the propagation mode of the detonation wave in a curved channel

transitioned from unstable to stable was having an inner radius of curvature of the curved channel

equivalent to 14 to 40 times the normal detonation cell width. They used the detonation cell width

from the Detonation Database (Kanesige and Shepherd [17], Abid et al. [18], Knystautas [19],

Strehlow [20]) of the California Institute of Technology to reduce their experimental data. They have

also proposed a formula which gives a geometrical front shock shape of a detonation wave

propagating through a curved channel at the CJ detonation velocity.

A simultaneous observation of the front shock shape of the detonation wave and the trajectories of

triple points on the detonation wave is ideal as a way to experimentally investigate the conditions of

a stable detonation wave propagating through a curved channel. We developed a new visualization

method to perform such a simultaneous observation and examined the conditions of the stable

detonation wave propagation in a curved channel by alternating the inner radius of the curved

channel and the filling pressure of the mixture gas parametrically. We also propose a formula which

gives a rigorous geometrical front shock shape for a detonation wave propagating stably through a

curved channel and examine the relation between the normal detonation velocity and the local

curvature of the detonation wave.

2. Geometric front shock shape of stable detonation wave in a curved channel

2.1 Geometric shape proposed by Kudo et al.

As shown in Fig. 1, the center of the inner/outer radius of curvature of a curved channel is defined

as the origin, and the boundary between the curved section and the straight section of the curved

channel is defined as the initial line in a two-dimensional polar coordinate system. The variable r

represents the distance from the origin, and θ is the angle from the initial line. If we assume that the

angular velocity of the detonation wave propagating stably through a curved channel is constant

everywhere on the detonation wave and the angular velocity is time-unvarying, the detonation wave

propagates through the curved channel while maintaining a specific shape [15]. If dr, dt, and $d\theta$ are

sufficiently small, one can consider the gray-colored areas in Fig. 1 to be right triangles. The

geometric relations can then be established at an arbitrary point P(r, θ) on the detonation wave,

$$\sin\phi = \frac{D_n}{r\omega},$$ (1)

$$\tan\phi = \frac{\sin\phi}{\sqrt{1-\sin^2\phi}} = -\frac{1}{r}\frac{dr}{d\theta},$$ (2)

where ϕ is the angular difference between the rotational direction and the tangential direction of the

detonation wave at P(r, θ), D_n is the normal detonation velocity at P(r, θ), and ω is the angular

velocity of the detonation wave. The following differential equation is derived from Eq. (1) and Eq.

(2):

$$\frac{d\theta}{dr} = -\frac{\sqrt{(r\omega)^2 - D_n^2}}{D_n r}.$$ (3)

If D_n is equal to the CJ detonation velocity (D_{CJ}) everywhere on the detonation wave and the

detonation wave is perpendicular to the inner wall of the curved channel, D_n is equal to the product

of the inner radius of curvature of the curved channel (r_i) and ω. Thus, the integration of Eq. (3)

gives a geometrical front shock shape of the detonation wave propagating through a curved channel

at a constant normal detonation velocity of D_{CJ} in terms of the relation between r and θ as follows

[15]:

$$\theta - \theta_i = -\sqrt{\left(\frac{r}{r_i}\right)^2 - 1} + \tan^{-1}\sqrt{\left(\frac{r}{r_i}\right)^2 - 1} \,, \qquad (4)$$

where θ_i is the angle from the initial line to the detonation wave front on the inner wall of the curved

channel. The front shock shape of the detonation wave given by Eq. (4) becomes independent of D_n

since D_n is assumed to be constant everywhere on the detonation wave.

The experiment by Kudo et al. [15] showed that D_n on the inner wall of the curved channel is

lower than D_{CJ} due to the expansion waves from the inner wall, even though the detonation wave

propagates stably in the curved channel. Hence, Eq. (4) is applicable only under the limited

condition of a sufficiently high filling pressure of mixture gas and a large inner radius of curvature of

the curved channel in which D_n becomes almost equivalent to D_{CJ}. Some modifications are

considered to be necessary in Eq. (4) to reconstruct the front shock shape of the detonation wave

propagating stably through a curved channel in other conditions. In order to derive a formula which

gives a rigorous geometrical front shock shape of the detonation wave under a wide range of

conditions, the deficit of D_n caused by the expansion waves from the inner wall should be taken into

account.

2.2 Geometric shape proposed in the present study

If the composition and temperature of the mixture gas are fixed, the velocity of the planar

detonation wave propagating through the straight section of a curved channel (D_{str}) and the normal

detonation cell width (λ) can be determined. Therefore, only the four variables, r_i, λ, r, and D_{str} are

considered to be the physical quantities which determine the value of D_n of the detonation wave

propagating stably through a curved channel. Therefore, D_n is expressed as a function of these

parameters as follows:

$$D_n = f_1\left(r_i, \lambda, r, D_{str}\right). \tag{5}$$

By using r_i, λ and r, we can define two significant dimensionless variables, r_i/λ and r/r_i. The

variable r_i/λ represents the ratio of the representative physical length scales of the flow field and

detonation wave, and the variable r/r_i represents the normalized front shock position of the

detonation waves. Considering that the physical dimensions of both sides of an equation need to be

equivalent, Eq. (5) may be reduced into the following dimensionless form by introducing these two

dimensionless variables:

$$\frac{D_n}{D_{str}} = f_2\left(\frac{r_i}{\lambda}, \frac{r}{r_i}\right). \tag{6}$$

If f_2 is determined, the following relation between r and θ, which gives the front shock shape of

the detonation wave propagating stably through a curved channel, is derived by substituting Eq. (6)

into Eq. (3) and integrating Eq. (3):

$$\theta - \theta_i = -\int_{r_i}^{r} \frac{\sqrt{(r\omega)^2 - D_n^2}}{D_n r}\, \mathrm{d}r \, . \tag{7}$$

Since $D_{n,i}$ is equal to $r_i\omega$, Eq. (7) can be reduced into the following equation:

$$
\begin{aligned}
\theta - \theta_i &= -\int_{r_i}^{r} \left\{ \left(\frac{r}{r_i}\right)^2 \left(\frac{D_{n,i}}{D_{str}}\right)^2 \left(\frac{D_n}{D_{str}}\right)^{-2} - 1 \right\}^{\frac{1}{2}} \left(\frac{1}{r}\right) \mathrm{d}r \\
&= -\int_{r_i}^{r} \left[\left(\frac{r}{r_i}\right)^2 \left\{ f_2\left(\frac{r_i}{\lambda}, \frac{r_i}{r_i}\right) \right\}^2 \left\{ f_2\left(\frac{r_i}{\lambda}, \frac{r}{r_i}\right) \right\}^{-2} - 1 \right]^{\frac{1}{2}} \left(\frac{1}{r}\right) \mathrm{d}r
\end{aligned}
\tag{8}
$$

That is to say, the front shock shape of the detonation wave can be determined if f_2, r_i and λ are given.

Generally, the local curvature of the detonation wave (κ) can be calculated from the following equation:

$$\kappa = \left\{ r^2 + 2\left(\frac{\mathrm{d}r}{\mathrm{d}\theta}\right)^2 - r\frac{\mathrm{d}^2 r}{\mathrm{d}\theta^2} \right\} \left\{ \left(\frac{\mathrm{d}r}{\mathrm{d}\theta}\right)^2 + r^2 \right\}^{-\frac{3}{2}} . \tag{9}$$

From Eq. (8), we can see that $\mathrm{d}r/\mathrm{d}\theta$ and $\mathrm{d}^2 r/\mathrm{d}\theta^2$ become a product of r and a function of r_i/λ and r_i/r.

Therefore, by substituting $\mathrm{d}r/\mathrm{d}\theta$ and $\mathrm{d}^2 r/\mathrm{d}\theta^2$ derived from Eq. (8) into Eq. (9), Eq. (9) can be reduced into a function of r_i/λ, r_i/r and r as follows:

$$\kappa = g_1\left(\frac{r_i}{\lambda}, \frac{r}{r_i}\right)\left(\frac{1}{r}\right) . \tag{10}$$

Eq. (10) can be reduced into the following dimensionless form by multiplying both sides of Eq. (10) by λ:

$$\lambda \kappa = g_1\left(\frac{r_i}{\lambda}, \frac{r}{r_i}\right)\left(\frac{\lambda}{r}\right)$$

$$= g_1\left(\frac{r_i}{\lambda}, \frac{r}{r_i}\right)\left(\frac{r_i}{\lambda}\right)^{-1}\left(\frac{r}{r_i}\right)^{-1}. \tag{11}$$

$$= g_2\left(\frac{r_i}{\lambda}, \frac{r}{r_i}\right)$$

The following equation is derived by solving Eq. (11) for r/r_i and substituting the equation into Eq.

(6):

$$\frac{D_n}{D_{str}} = h\left(\frac{r_i}{\lambda}, \lambda\kappa\right). \tag{12}$$

The bottom line is that the front shock shape of the detonation wave and the relation between D_n/D_{str}

and r_i/λ or between D_n/D_{str} and $\lambda\kappa$ can be derived if f_2 is determined.

The expansion waves from the inner wall of the curved channel decrease D_n since the expansion

waves diffract the detonation wave. The influence of the expansion waves is the strongest on the

inner wall and becomes negligible at a distance sufficiently far away from the inner wall. Therefore,

we can suppose that D_n becomes the smallest on the inner wall of the curved channel where the

influence of the expansion waves becomes the strongest. We can also suppose that D_n increases as if

to approach asymptotically to a certain value at a distance sufficiently far from the inner wall since

the influence of the expansion waves decrease with distance from the inner wall. As a formula that

gives approximately such D_n characteristics, we propose the following formula which is a

phenomenological dependence:

$$\frac{D_\text{n}}{D_\text{str}} = \frac{D_\text{n,asy}}{D_\text{str}} - \left(\frac{D_\text{n,asy}}{D_\text{str}} - \frac{D_\text{n,i}}{D_\text{str}}\right)\left(\frac{r}{r_\text{i}}\right)^{-m}, \qquad (13)$$

where $D_\text{n,asy}$ and m are constant, and $D_\text{n,asy}$ is the asymptotic value of D_n at a distance sufficiently far

from the inner wall. The influence of r_i and λ on D_n is expressed by these three constants, $D_\text{n,asy}$, $D_\text{n,i}$,

and m. D_n increases from $D_\text{n,i}$ to $D_\text{n,asy}$ asymptotically with increasing r in Eq. (13). $D_\text{n,i}$ and D_n at

arbitrary points on the detonation wave are preliminarily acquired at a given r_i and λ in an

experiment. $D_\text{n,asy}$ and m are determined by applying the least-square method to the experimental $D_\text{n,i}$

using Eq. (13). Although one can assume that $D_\text{n,asy}/D_\text{str} = 1$ at a distance sufficiently far from the

inner wall, we determined $D_\text{n,asy}$ by the least-square method in order to increase the flexibility and

accuracy of the approximation in the vicinity of the inner wall in the present study.

If a detonation wave propagates stably through a curved channel while maintaining a specific

shape at a constant angular velocity, D_n can be determined from Eq. (3). The following equation is

obtained by solving Eq. (3) for D_n:

$$D_\text{n} = -r\omega\left(\frac{1}{r}\frac{\text{d}r}{\text{d}\theta}\right)\Bigg/\sqrt{\left(\frac{1}{r}\frac{\text{d}r}{\text{d}\theta}\right)^2 + 1}. \qquad (14)$$

The value of $\text{d}r/\text{d}\theta$ in Eq. (14) is approximately obtained by the Taylor series expansion of r with

respect to θ and by neglecting high-order terms. By taking into account the terms to the second-order,

$\text{d}r/\text{d}\theta$ is discretely approximated by the following equation:

$$\left(\frac{\mathrm{d}r}{\mathrm{d}\theta}\right)_k \approx \left\{ r_{k+1} - r_k - \frac{1}{2}\left(\frac{\mathrm{d}^2 r}{\mathrm{d}\theta^2}\right)_k (\theta_{k+1} - \theta_k)^2 \right\} \bigg/ (\theta_{k+1} - \theta_k). \qquad (15)$$

$\mathrm{d}^2 r/\mathrm{d}\theta^2$ can also be discretely approximated using the following equation:

$$\left(\frac{\mathrm{d}^2 r}{\mathrm{d}\theta^2}\right)_k \approx \left(\frac{r_{k+1} - r_k}{\theta_{k+1} - \theta_k} - \frac{r_k - r_{k-1}}{\theta_k - \theta_{k-1}}\right) \bigg/ \left(\frac{\theta_{k+1} - \theta_k}{2} + \frac{\theta_k - \theta_{k-1}}{2}\right). \qquad (16)$$

If the interval of θ is constant, Eq. (16) is the so-called second-order accurate central-difference of r

with respect to θ. By recording the detonation wave shape at an arbitrary time interval and dividing

it at a regular interval as shown in Fig. 1, one can pick up the coordinate values of the points of

division and obtain the ω of each point by observing the alternation of their positions from moment

to moment. If the ω values of each point are equivalent to each other and are time-unvarying, the

values of D_n on the points of division are determined from Eqs. (14)-(16) using the ω and the

coordinate values of the points of division.

Since Eq. (7) and Eq. (13) give the front shock shape of the detonation wave as a continuous

function of r and θ, κ can be calculated from Eq. (9). $\mathrm{d}r/\mathrm{d}\theta$ and $\mathrm{d}^2 r/\mathrm{d}\theta^2$ are derived from Eq. (3) and

the derivative of Eq. (3) with respect to θ, respectively.

3. Visualization method

3.1 Short-time open-shutter photography (SOP)

The front shock shape of the detonation wave propagating through a curved channel and the

14

trajectories of triple points on the detonation wave were simultaneously recorded by Short-time

Open-shutter Photography (SOP). The concept of SOP is shown in Fig. 2. A detonation wave is

propagating through a curved channel from the lower right to the upper left and is recorded by SOP

at an exposure time of Δt in Fig. 2. By limiting the exposure time to a few microseconds, only the

triple point trajectories within the area swept by the detonation wave front are recorded in the

exposure time. The forward or backward edges of the triple point trajectories recorded in the SOP

image give the front shock shape of the detonation wave of the moment. The influence of the

luminescence of burned gas can also be minimized in the SOP image by setting the exposure time

appropriately.

3.2 Multi-frame short-time open-shutter photography (MSOP)

By performing SOP for each individual frame of a high-speed camera, the image of the overall

triple point trajectories in a curved channel is visualized from the superimposition of these SOP

images. This new visualization method is named Multi-frame Short-time Open-shutter Photography

(MSOP) in the present study.

4. Experimental setup and conditions

The schematics of the curved channels and observation chamber used in the present study are

shown in Fig. 3. Five types of curved channels with different inner radii of curvature (5 mm, 10 mm, 20 mm, 40 mm, and 60 mm) were used. The cross-section of these channels is rectangular and the width is 20 mm. The depth of these channels is set very thin (1 mm) so that the structures of the detonation waves propagating through the channels become two-dimensional. Thus, the trajectories of the triple points can be recorded clearly by MSOP.

The observation chamber consists of circular-cross-section tubes of 25.8 mm in diameter, rectangular-cross-section tubes of 20 mm x 16 mm, and a curved channel. The mixture gas filled in the observation chamber is ignited by a spark plug mounted at the closed end of the circular-cross-section tube below the curved channel. A deflagration wave transitions to a detonation wave within the Shchelkin spiral section mounted in the tube. The detonation wave enters the curved channel via the rectangular-cross-section tube. A low-vacuum dump tank of 0.037 m^3 is connected to the outlet port of the observation chamber, and a mylar film separates the dump tank and the observation chamber. The detonation wave passing through the curved channel ruptures the film, and the high pressure and temperature gas generated by the detonation wave is caught in the dump tank.

A stoichiometric ethylene-oxygen mixture gas was used in the present study. The mixture gas is filled at a given pressure into the observation chamber in which the air is evacuated. The temperature of the mixture gas is equal to the room temperature. The experimental conditions are summarized in Table 1, where p_0 is the filling pressure of the mixture gas and T_0 is the temperature of mixture gas.

The images of the detonation waves propagating through the curved channels were taken by a high-speed video camera (Shimadzu HPV-2) through an observation window of 120 mm in diameter. All the images were taken at 4-μs time intervals in each experiment. The spatial resolution of the images is 0.3 mm. The output voltage of the piezoelectric transducer mounted near the closed-end of the circular-cross-section tube below the curved channel was used as a trigger to start shooting by the high-speed camera.

5. Stable and unstable detonation waves in a curved channel

5.1 Planarity and speed of detonation wave in a straight section

The positions of the detonation wave propagating through the straight section of a curved channel were determined from an MSOP image. It was verified that the detonation wave in the straight section was planar since the forward edge of the triple point trajectories recorded was quite straight. Figure 4 shows the measurement results of D_{str}. The symbols are the averages of three values measured at 4-μs time intervals and the solid line is D_{CJ} calculated using CEA [21]. The error bars represent the ranges of minimum-to-maximum deviation and the systematic error of the measured values. All the values of measured D_{str} were 5% lower than D_{CJ}. This velocity deficit was considered to have been caused by the thin depth (1 mm) of the curved channels, which forces the detonation structure to be two-dimensional.

5.2 Detonation cell width

The value of λ of the detonation wave propagating through the straight section of a curved

channel was measured from an MSOP image. The measurement of λ was conducted under

conditions in which the filling pressure of the mixture gas was relatively low; that is to say, the

detonation cell width became large (Shot No. 15, Shot No. 16, Shot No.24). Figure 5 shows the

measurement results of λ. The values of the detonation cell width on the Detonation Database of the

California Institute of Technology [17-20] are also shown in Fig. 5. In Fig. 5, the measured value in

the present study is the average of ten values measured arbitrarily within the straight section. The

error bars represent the ranges of minimum-to-maximum deviation of the measured values. The

measurement results of λ in the present study did not contradict those of other studies [17-20]. The

relation of $\lambda = 70.020 \times p_0^{-1.1270}$ could be obtained by applying the least-square method to all the data

shown in Fig. 5.

5.3 Detonation propagation characteristics in a curved channel

The value of $D_{n,i}$ was measured from the alternation of the forward edge position of the

luminescence region on the inner wall as determined using the MSOP image. The propagation of the

detonation wave through a curved channel was categorized based on how high $D_{n,i}$ was. The typical

histories of $D_{n,i}$ are shown in Fig. 6. $D_{n,i}$ is nondimensionalized by D_{str} in Fig. 6. The error bars of the

rightmost symbols represent the ranges of systematic error of measurement. In the present study, the

propagation mode that consistently satisfies the relation of $D_{n,i}/D_{str} \geq 0.8$ is defined as the stable

mode, the mode that cannot satisfy the relation of $D_{n,i}/D_{str} \geq 0.8$ but can consistently satisfy the

relation of $D_{n,i}/D_{str} \geq 0.6$ is defined as the critical mode, and the mode in which $D_{n,i}/D_{str} < 0.6$ even

just once is defined as the unstable mode. In Fig. 6, circles correspond to the stable mode, triangles

to the critical mode, and crosses to the unstable mode.

As shown in Fig. 6, the variation range of $D_{n,i}/D_{str}$ is narrow in the case of the stable mode,

therefore we can consider the detonation wave in the stable mode to be the so-called steady

detonation wave. On the other hand, the variation range of $D_{n,i}/D_{str}$ is wide in the case of the unstable

mode. Therefore, we can consider the detonation wave in the unstable mode to be the so-called

unsteady detonation wave. The detonation wave in the critical mode may be the intermediate

between the steady and unsteady detonation waves.

The typical MSOP images taken at a given r_i ($r_i = 40$ mm) are shown in Fig. 7. The images in Fig.

7 were taken in the same experiments represented in Fig. 6. The arrows in Fig. 7 show the

propagation direction of the detonation wave. Fig. 7(a) corresponds to the stable mode, Fig. 7(b) to

the critical mode, and Fig. 7(c) to the unstable mode. At a given r_i, a higher p_0 makes the detonation

wave in a curved channel more stable.

The detonation cell in the vicinity of the inner wall of the curved channel is enlarged soon after the

19

detonation wave enters the curved section of the channel due to the expansion waves from the inner

wall as shown in Fig. 7(a). When the cell has enlarged to about twice its normal size, new cells are

generated smoothly within the enlarged cells in the vicinity of the inner wall. The smooth detonation

wave front can be maintained consistently in the stable mode due to this smooth cell generation. It is

possible that $D_{n,i}/D_{str}$ is maintained consistently above 0.8 in the stable mode in Fig. 6 due to this

smooth cell generation. The detonation wave propagates while maintaining a specific shape, and the

interval of the detonation wave front recorded in the MSOP image is constant within $\theta_i = 45$-90 deg.

In the critical mode, the cell in the vicinity of the inner wall is also enlarged soon after the

detonation wave enters the curved section as shown in Fig. 7(b). Although the collapse of the

detonation cell structure has not yet been observed, the cell has increased to about three times its

normal size within $\theta_i = 60$-90 deg. $D_{n,i}/D_{str}$ may fall below 0.8 in the critical mode in Fig. 6 due to

this significant cell enlargement in the vicinity of the inner wall. The interval of the detonation wave

front recorded in the MSOP image is not constant in the region where significant cell enlargement is

observed.

A collapse of the detonation cell structure occurs in the unstable mode. A temporary collapse of

the detonation cell structure is observed in the vicinity of the inner wall around $\theta_i = 35$ deg in Fig.

7(b). Although the detonation cell structure in the vicinity of the inner wall is recovered from around

$\theta_i = 45$ deg by the generation of new fine cells, the detonation cell structure collapses completely

within θ_i = 70-90 deg. It is possible that the detonation wave has once transitioned to the deflagration

wave in such a region and that $D_{n,i}/D_{str}$ falls below 0.4 in the unstable mode in Fig. 6 due to this

complete collapse of the detonation cell structure.

The typical MSOP images taken at a given p_0 (p_0 = 31.0 ±1.0 kPa) are shown in Fig. 8. Fig. 8(a)

corresponds to the stable mode, Fig. 8(b) to the critical mode, and Figs. 8(c)-(e) to the unstable mode.

At a given p_0, a larger r_i makes the detonation wave more stable. That is to say, the increase of r_i has

the same effect as the increase of p_0 on the stability of the detonation wave in a curved channel.

5.4 Condition of stable detonation propagation in a curved channel

The relation between r_i and λ is shown in Fig. 9 in terms of the propagation mode of the

detonation wave propagating through a curved channel. At a given λ, a larger r_i makes the detonation

wave more stable. A smaller λ also makes the detonation wave more stable at a given r_i. From this

result, we can see that the smaller the inner radius of the annular combustor of RDE is, the smaller λ

(or the higher p_0) is required for the stable operation of RDE. The stable operation range of p_0 for

RDE may be expanded by increasing the inner radius of the annular combustor of RDE.

In Fig. 9, one can see that the stable mode and critical mode as well as the critical mode and

unstable mode may be separated by a line of r_i/λ = const. Therefore, we defined the stable zone,

transitional zone, and unstable zone based on how high r_i/λ was. The zone where the stable mode is

consistently attained above a line of r_i/λ = const. is defined as the stable zone and the line is the

threshold of the stable zone. The zone where no unstable mode is observed above a line of r_i/λ =

const. but below the threshold of the stable zone is defined as the transitional zone and the line is the

threshold of the transitional zone. The remaining zone is defined as the unstable zone. We altered the

value of r_i/λ at the interval of 1 and found that r_i/λ = 32 and 21 were the thresholds of the stable zone

and transitional zone, respectively. Therefore, the propagation mode of the detonation wave is

considered to transition to the stable mode from the unstable mode within $21 \leq r_i/\lambda \leq 32$ in the

present study.

6. D_n-κ relation of stable detonation wave in a curved channel

The motion of the detonation wave propagating through a curved channel is analyzed under the

condition of $r_i/\lambda \geq 32$ where the propagation mode of the detonation wave is consistently stable. The

cases of the analysis are shown in Table 2. The detonation cell width of these cases is 0.6 mm. The

front shock shape of the detonation wave is quantified by dividing it into 15 parts at a regular

interval as shown in Fig. 1 and picking up the coordinate values of the points of division. The ranges

of θ_i where the transition from a planar detonation wave to a fully-developed curved detonation

wave was observed (θ_{trans}) are also shown in Table 2. If θ_i becomes larger than θ_{trans}, the detonation

wave takes a specific shape and the shape becomes steady. Therefore, three images in which the

detonation wave being close to the exit of the curved section was recorded were selected to pick up

the coordinate values in order to analyze the motion of the detonation wave of which the shape was

quite steady.

6.1 Angular velocity of stable detonation wave in a curved channel

The relation between ω and r-r_i is shown in Fig. 10. The error bars of the symbols represent the

ranges of systematic error of measurement. ω increases with decreasing r_i. In all of the cases in the

analysis, ω is constant everywhere on the detonation wave and is time-unvarying.

Since a detonation wave is self-sustaining, the detonation wave which is once decelerated by an

expansion wave has an ability to recover its velocity again to D_{CJ} if the detonation wave is not

quenched by the expansion wave. In the case of the detonation wave propagating stably through a

curved channel, expansion waves are continuously generated from the inner wall of the curved

channel as long as the detonation wave continues propagating, and they forces the detonation wave

to decrease its velocity. From the results shown in Fig. 10, we can suppose that these two effects, the

accelerating effect which the decelerated detonation wave has and the decelerating effect by

expansion waves, balances on the inner wall of the curved channel since the value of ω becomes

time-invariant.

Figure 11 shows the schematic of the behavior of the stable detonation wave in a curved channel.

In figure 11, the solid line represents the front shock of the detonation wave, the dashed line

represents the particle path which is perpendicular to the front shock, and the dashed-dotted line

represents the expansion wave, respectively. On the inner wall of the curved channel, $D_n = r_i\omega$ and

the particle path is along the inner wall. Now, we focus our attention on the point $P(r_i+\delta r,\ \theta-\delta\theta)$ at a

distance infinitely close to the inner wall ($\delta r, \delta\theta << 1$). Since the point P is not on the inner wall and

ω is time-invariant, the particle path from the point P is not along the inner wall and D_n is nearly

equal to $r_i\omega$ at the point P regardless of θ_i. The particle path gradually gets away from the inner wall

as the detonation wave propagates, and finally it reaches the outer wall of the curved channel. D_n

increases gradually from the value of $r_i\omega$ along the particle path. Since r_i is constant, the conditions

of expansion waves are also constant regardless of θ_i. Therefore, the degree of the influence of the

expansion waves on the particle path is constant at any θ_i, and thus the shape of the particle path and

the distribution of D_n on the particle path do not change with the value of θ_i. Consequently, the value

of D_n and its direction become constant on the line of $r =$ const. This property may make the front

shock shape of the detonation wave steady. Therefore, the value of ω becomes constant everywhere

on the detonation wave as shown in Fig. 10.

6.2 Normal propagation speed of stable detonation wave in a curved channel

The relation between D_n/D_{str} and r-r_i is shown in Fig. 12. The symbols represent the average of the

measured values of D_n of each point of division on the three detonation wave fronts corresponding to

each θ_i shown in Table 2. The error bars of the symbols represent the ranges of

minimum-to-maximum deviation of the measured values. $D_{n,i}$ becomes the smallest among the

normal detonation velocities on the detonation wave and decreases with decreasing r_i/λ. D_n increases

as if to approach asymptotically to a certain value with increasing r-r_i. The solid line in Fig. 12 is

drawn by Eq. (13) and is in good agreement with the measured D_n. Hence, Eq. (13) is considered to

be an appropriate formula which approximately gives the relation between D_n and r on the

detonation wave at a given r_i and λ. The relations between $D_{n,asy}$ and r_i/λ and between m and r_i/λ are

shown in Fig. 13. $D_{n,asy}$ is nondimensionalized by D_{str} in Fig. 13. Since $D_{n,asy}$ is almost equivalent to

D_{str} under the condition of $r_i/\lambda \geq 67.3$, one can consider $D_{n,asy}/D_{str} = 1$ if r_i/λ is sufficiently large.

However, as $D_{n,asy}$ tends to be smaller than D_{str} under the condition of a smaller r_i/λ, one should

determine $D_{n,asy}$ by the least-square method in such a condition. The parameter m increases with

increasing r_i/λ in a linear manner.

The experimental and reconstructed front shock shapes of the detonation waves, which are

expressed by r-θ relations, are shown in Fig. 14. The symbols represent the average positions of each

point of division on the three detonation wave fronts corresponding to each θ_i shown in Table 2. The

error bars represent the ranges of minimum-to-maximum deviation and systematic error of the

measured values. The solid line is the front shock shape of the detonation wave reconstructed using

Eq. (7) and Eq. (13). The dashed-dotted line is the one reconstructed by using Eq. (4). The shape of

the detonation wave reconstructed by using Eq. (7) and Eq. (13) agrees much better with the

experimental result in all of the analysis cases than the one reconstructed by using Eq. (4) does. The

result shown in Fig. 14 also shows that Eq. (13) is an appropriate formula for giving D_n

approximately.

6.3 D_n-κ relation

The relation between $\lambda\kappa$ and $(r-r_i)/\lambda$ derived from the reconstructed front shock shape of the

detonation wave is shown in Fig. 15. $\lambda\kappa$ decreases with increasing $(r-r_i)/\lambda$. The largest $\lambda\kappa$ is

observed on the inner wall of the curved channel and increases with increasing r_i/λ.

The relation between D_n/D_{str} and $\lambda\kappa$ is shown in Fig. 16. D_n/D_{str} decreases with increasing $\lambda\kappa$.

This nondimensionalized D_n-κ relation is nearly independent of the r_i/λ. The D_n-κ relation, in which

D_n and κ are nondimensionalized by D_{CJ} and the induction zone length scale respectively, has been

examined theoretically by steady or quasi-steady one-dimensional analyses [22-25]. These analyses

have shown that D_n is a function of only κ in one-dimensional ZND detonation. The present study

has experimentally shown that D_n/D_{str} of a stoichiometric ethylene-oxygen mixture gas is also a

function of only $\lambda\kappa$, as in the theoretical studies.

However, the evaluation of the D_n-κ relation in the present study is limited to a certain high filling

pressure condition of the mixture gas. Therefore, the D_n-κ relation is not yet proven to be universal.

Further evaluation of the D_n-κ relation throughout the stable zone shown in Fig. 9 is required in

order to confirm that the D_n-κ relation is universal or not. However, it is difficult to define the front

shock shapes of the detonation waves precisely from MSOP images under the low filling pressure

conditions of the mixture gas. Therefore, we need the other visualization experiments employing

another method specialized for the visualization of the front shock shapes in order to perform the

further evaluation of the D_n-κ relation.

6. Conclusions

The detonation propagation phenomena in curved channels were experimentally studied in order

to examine the stable propagation condition. A stoichiometric ethylene-oxygen mixture gas and five

types of rectangular-cross-section curved channels with different inner radii of curvature were used.

The inner radius of curvature of the curved channel (r_i) and the filling pressure of the mixture gas

(p_0), that is to say, the normal detonation cell width (λ), were parametrically altered. The front shock

shapes of detonation waves propagating through the curved channels and the trajectories of triple

points on the detonation waves were simultaneously observed using Multi-frame Short-time

Open-shutter Photography (MSOP), and the following results were obtained.

When the detonation wave propagation in a curved channel was in the stable mode ($r_i/\lambda \geq 32$),

new detonation cells were generated smoothly within the enlarged cells in the vicinity of the inner

wall of the curved channel. This smooth cell generation consistently maintained the smooth

detonation wave front in the stable mode. At a given r_i, a higher p_0 made the detonation wave more

stable. And at a given p_0, a larger r_i also made the detonation wave more stable. The propagation

mode of the detonation wave was considered to transition to the stable mode from the unstable mode

within $21 \leq r_i/\lambda \leq 32$.

The normal detonation velocity (D_n) increased with distance from the inner wall and approached

the velocity of the planar detonation entering the curved section of the curved channel (D_{str}). The

smallest D_n was observed on the inner wall of the curved channel and decreased with decreasing r_i/λ.

The distribution of D_n on the detonation wave in the stable mode was approximately formulated. The

approximated D_n given by the formula agreed well with the experimental results. The front shock

shape of the detonation wave could be reconstructed accurately using the formula.

The local curvature of the detonation wave (κ) nondimensionalized by λ decreases with increasing

distance from the inner wall of the curved channel. The largest $\lambda\kappa$ was observed on the inner wall of

the curved channel and increased with increasing r_i/λ. D_n/D_{str} decreased with increasing $\lambda\kappa$. This

nondimensionalized D_n-κ relation was nearly independent of r_i/λ.

In the present study, the stable condition of the detonation wave propagating through curved

channels was determined by using the two-dimensional curved channels. Since the actual

propagation of the detonation wave in the annular combustor of RDE is three-dimensional and

another curvature may exist on the front shock of the detonation wave, its application to RDE may

be limited even if a stoichiometric ethylene-oxygen mixture gas is employed as its propellant. The

local curvature of the detonation wave may affect the stability of the detonation wave, however the

relation between the local curvature and the stability of the detonation wave has not been revealed

yet in the present study. Therefore, we need further experimental investigation in order to elucidate

this relation.

Acknowledgements

H. Nakayama, T. Moriya, J. Kasahara, A. Matsuo, and I. Funaki, Combustion and Flame, Vol. 159 (2012) pp. 859-869.

References

[1] E. M. Braun, N. D. Dunn, F. K. Lu, Testing of a Continuous Detonation Wave Engine with

Swirled Injection, AIAA 2010-146.

[2] J. Meredith, H. Ng, L. H. S. Lee, Proc. 22nd ICDERS, paper 64, 2009.

[3] J. Kindracki, P. Wolański, Z. Gut, Proc. 22nd ICDERS, paper 76, 2009.

[4] M. Hishida, T. Fujiwara, P. Wolanski, Shock Waves (19) (2009) 1-10.

[5] F. Falempin, E. Daniau, A Contribution to the Development of Actual Continuous Detonation

Wave Engine, AIAA 2008-2679.

[6] N. Tsuboi, S. Adachi, K. Hayashi, E. Yamada, M. Uchida, T. Fujimori, T. Suda, J. Combust. Soc.

Japan 52 (161) (2010) 213-223.

[7] Z. Liang, T. Curran, J. E. Shepherd, Technical Report FM2006-008, GALCIT, 2006.

[8] Z. Liang, T. Curran, J. E. Shepherd, Proc. 26th ISSW 1, 2007, p. 383-388.

[9] D. H. Edwards, G. O. Thomas, M. A. Nettleton, Archivum Combustionis 3 (1) (1983) 65-76.

[10] G. O. Thomas, R. L. Williams, Shock Waves 11 (2002) 481-492.

[11] S. M. Frolov, V. S. Aksenov, I. O. Shamshin, Proc. Combust. Inst. 31 (2006) 2421-2428.

[12] S. M Frolov, V. S. Aksenov, I. O. Shamshin, J. Loss Prevent. Proc. Ind. 20 (2007) 501-508.

[13] S. M. Frolov, V. S. Aksenov, I. O. Shamshin, Dokl. Phys. Chem. 418 (2) (2008) 22-25.

[14] S. M. Frolov, V. S. Aksenov, I. O. Shamshin, Russ. J. Phys. Chem. B 2 (5) (2008) 759-774.

H. Nakayama, T. Moriya, J. Kasahara, A. Matsuo, and I. Funaki,
Combustion and Flame, Vol. 159 (2012) pp. 859-869.

[15] K. Kudo, Y. Nagura, J. Kasahara, Y. Sasamoto, A. Matsuo, Proc. Combust. Inst. 33 (2010) (in

press).

[16] Y. Sasamoto, A. Matsuo, J. Kasahara, Proc. 48th Symposium (Japan) on Combustion (2010)

492-493.

[17] M. Kaneshige, J. E. Shepherd, Technical Report FM97-8, GALCIT, 1997.

[18] S. Abid, G. Dupre, C. Paillard, Prog. Astronaut. Aeronaut. 153 (1991) 162-181.

[19] R. Knystautas, J. H. S. Lee, C. M. Guirao, Combust. Flame 48 (1982) 63-83.

[20] R. A. Strehlow, AIAA J. 7 (3) (1969) 492-496.

[21] S. Gordon, B. J. McBride, NASA Reference Publication 1311, 1994.

[22] J. B. Bdzil, J. Fluid Mech. 108 (1981) 195-226.

[23] R. Klein, D. S. Stewart, SIAM J. Appl. Math. 53 (1993) 1401-1435.

[24] D. S. Stewart, J. B. Bdzil, Combust. Flame 72 (1988) 311-323.

[25] J. Yao, D. S. Stewart, Combust. Flame 100 (1995) 519-528.

Table 1. Experimental conditions ($T_0 = 298 \pm 1$ K).

Shot No.	p_0 [kPa]	r_i [mm]	λ [mm]	D_{str} [m/s]	Propagation mode
1	21.0	5	2.3	2183.3	Unstable
2	31.0	5	1.5	2232.3	Unstable
3	41.0	5	1.1	2207.8	Unstable
4	51.0	5	0.9	2232.3	Unstable
5	61.0	5	0.7	2281.4	Unstable
6	70.6	5	0.6	2281.4	Unstable
7	80.6	5	0.5	2305.9	Unstable
8	21.0	10	2.3	2177.9	Unstable
9	31.0	10	1.5	2226.9	Unstable
10	41.0	10	1.1	2226.9	Unstable
11	51.0	10	0.9	2251.3	Unstable
12	61.0	10	0.7	2275.8	Unstable
13	70.6	10	0.6	2275.8	Critical
14	80.6	10	0.5	2300.3	Critical
15	20.3	20	2.4	2143.5	Unstable
16	30.3	20	1.5	2192.8	Unstable
17	36.5	20	1.2	2188.8	Unstable
18	40.3	20	1.1	2217.4	Unstable
19	45.3	20	1.0	2242.0	Unstable
20	50.3	20	0.9	2266.7	Critical
21	60.3	20	0.7	2291.3	Critical
22	70.3	20	0.6	2315.9	Stable
23	20.8	40	2.4	2139.3	Unstable
24	25.8	40	1.8	2188.5	Critical
25	31.5	40	1.5	2195.1	Critical
26	36.5	40	1.2	2219.5	Stable
27	40.8	40	1.1	2213.1	Stable
28	50.8	40	0.9	2237.7	Stable
29	60.8	40	0.7	2262.3	Stable
30	70.6	40	0.6	2277.6	Stable
31	20.8	60	2.4	2121.2	Critical
32	26.5	60	1.8	2212.4	Stable
33	28.5	60	1.7	2212.4	Stable
34	30.8	60	1.5	2212.1	Stable
35	40.8	60	1.1	2242.4	Stable
36	50.8	60	0.9	2242.4	Stable
37	60.8	60	0.7	2272.7	Stable
38	70.8	60	0.6	2272.7	Stable

Table 2. Analysis cases of the motion of the stable detonation wave in a curved channel.

Shot No.	r_i/λ [-]	θ_i [deg]	θ_{trans} [deg]
22	33.5	116.6, 139.5, 162.1	71.3-93.8
30	67.3	59.3, 71.6, 84.0	47.3-59.3
38	101.3	68.5, 76.8, 85.2	43.5-52.0
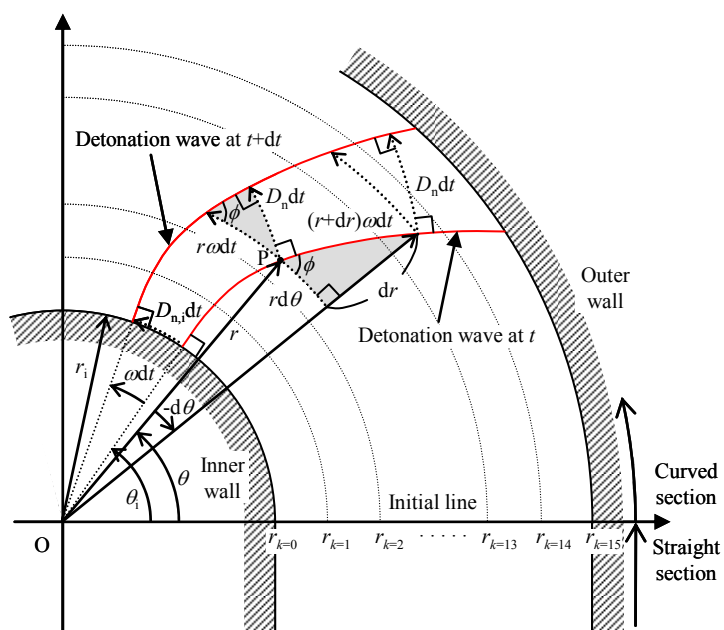
Fig. 1. Geometric relationship in a stable detonation wave propagating through a rectangular

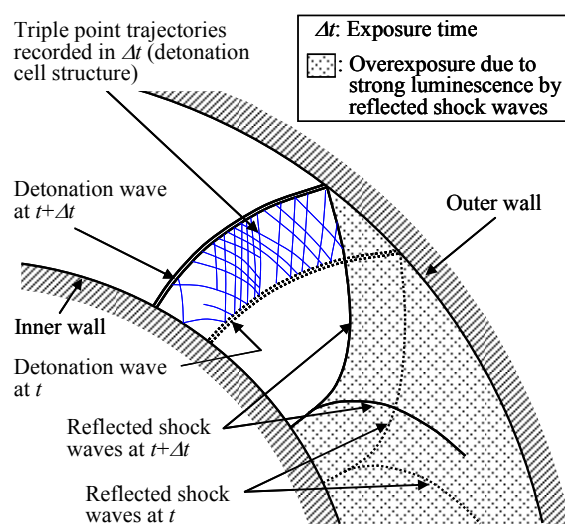cross-section curved channel with constant inner/outer curvature radii.

Triple point trajectories
recorded in *Δt* (detonation
cell structure)

Δt: Exposure time

: Overexposure due to
strong luminescence by
reflected shock waves

Detonation wave
at *t+Δt*

Outer wall

Inner wall

Detonation wave
at *t*

Reflected shock
waves at *t+Δt*

Reflected shock
waves at *t*

Fig. 2. Schematic illustrating the concept of Short-time Open-shutter Photography (SOP).

(1) r_i=5 mm   (2) r_i=10 mm   (3) r_i=20 mm

(4) r_i=40 mm   (5) r_i=60 mm

(a) Curved channels

(b) Observation chamber
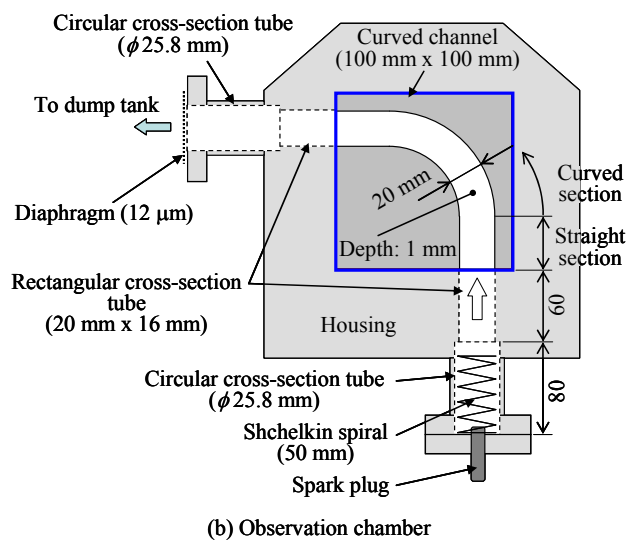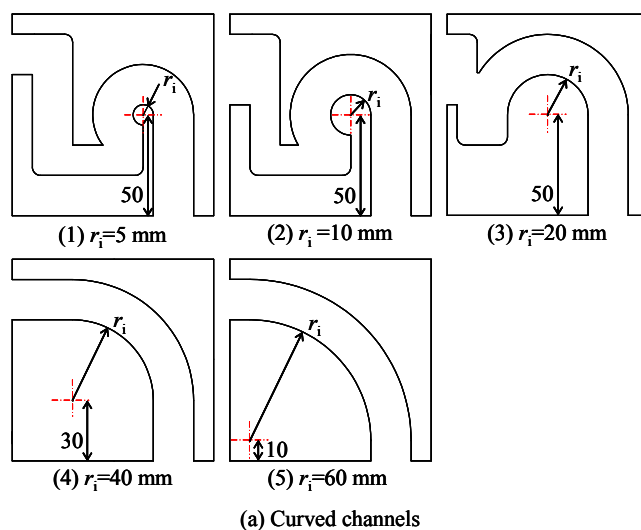
Fig. 3. Schematic of the channels and observation chamber.
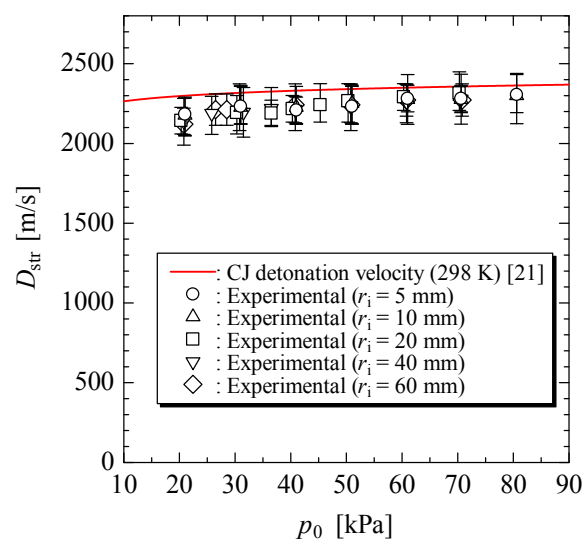
Fig. 4. Velocity of the planar detonation wave propagating through the straight section of a curved
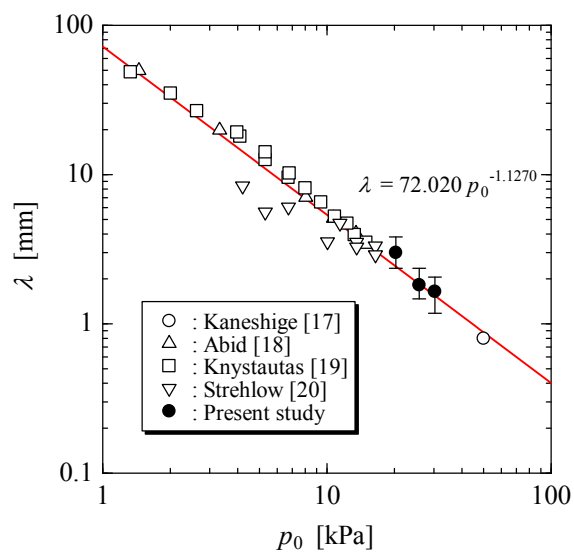
channel.

Fig. 5. Detonation cell width of the planar detonation wave propagating through the straight section
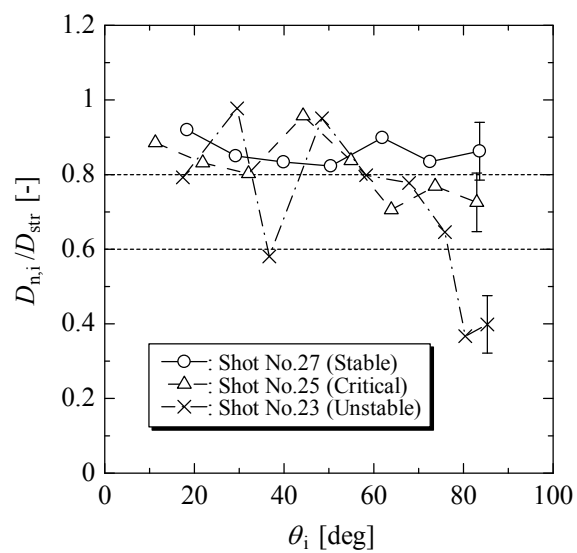
of a curved channel.

Fig. 6. Typical histories of the normal detonation velocity on the inner wall of a curved channel.
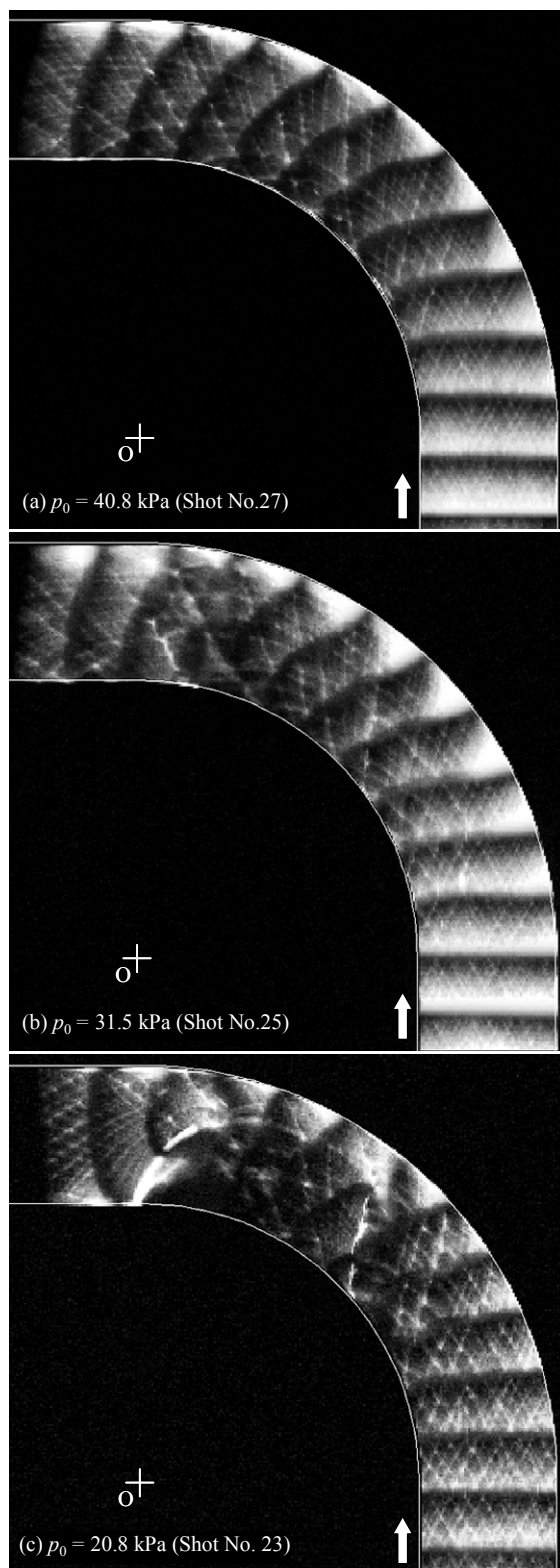
Fig. 7. Typical images of Multi-frame Short-time Open-shutter Photography (MSOP) at a given

inner radius of a curved channel (r_i = 40 mm).
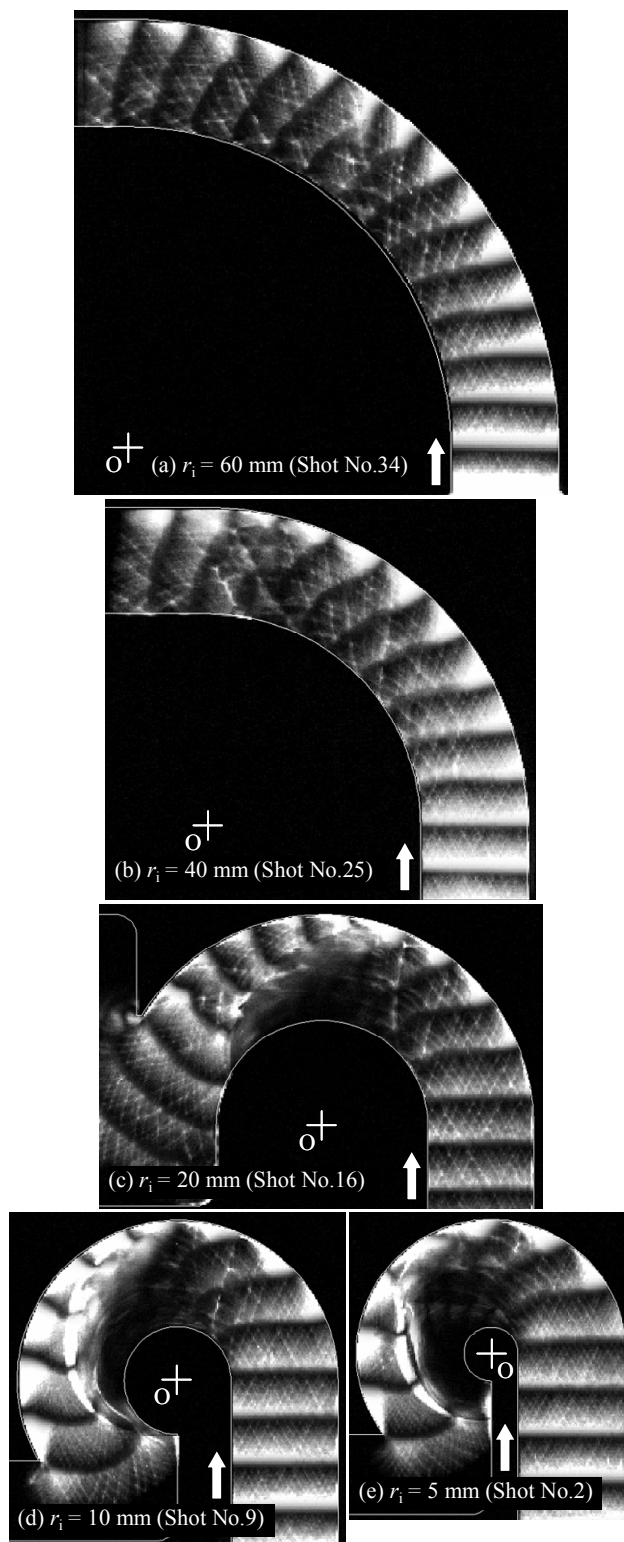
Fig. 8. Typical images of Multi-frame Short-time Open-shutter Photography (MSOP) at a given

filling pressure of mixture gas (p_0 = 31.0 ±1.0 kPa).
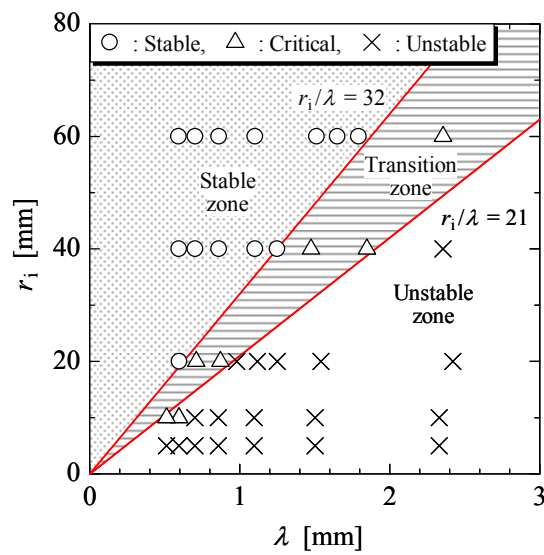
Fig. 9. Relation between the inner radius of the curved channel and the normal detonation cell width

in terms of the propagation mode of the detonation wave propagating through a curved channel.
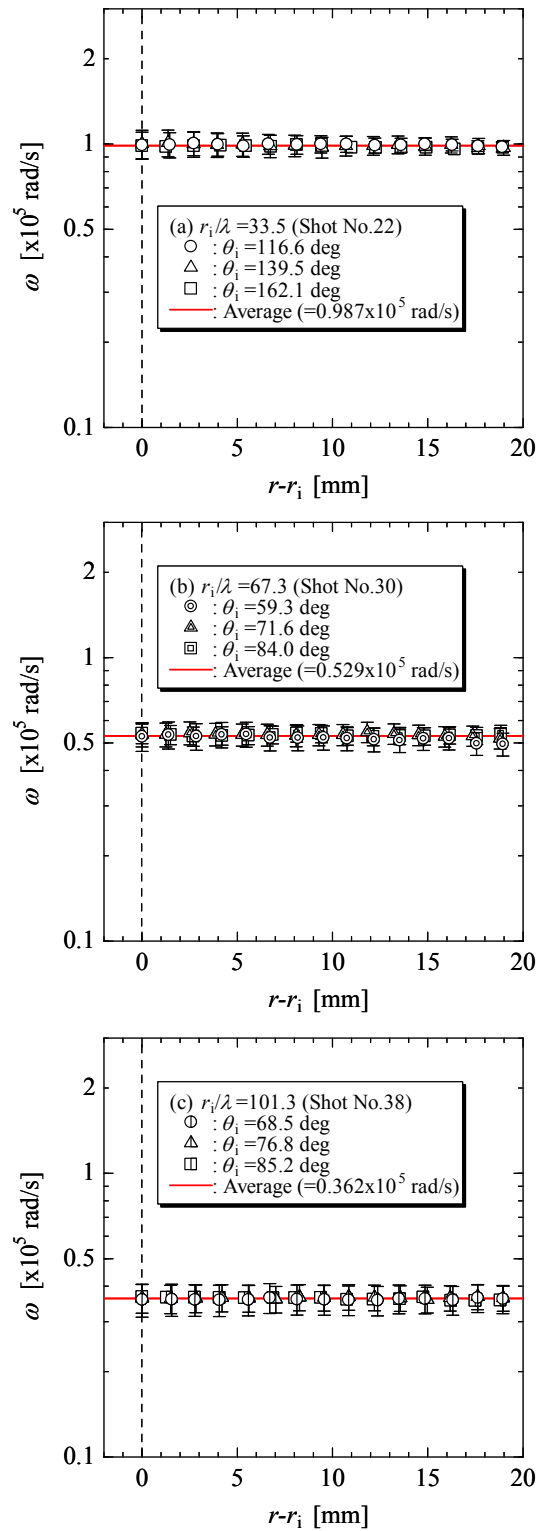
Fig. 10. Distribution of the angular velocity on the detonation wave in the stable propagation mode.
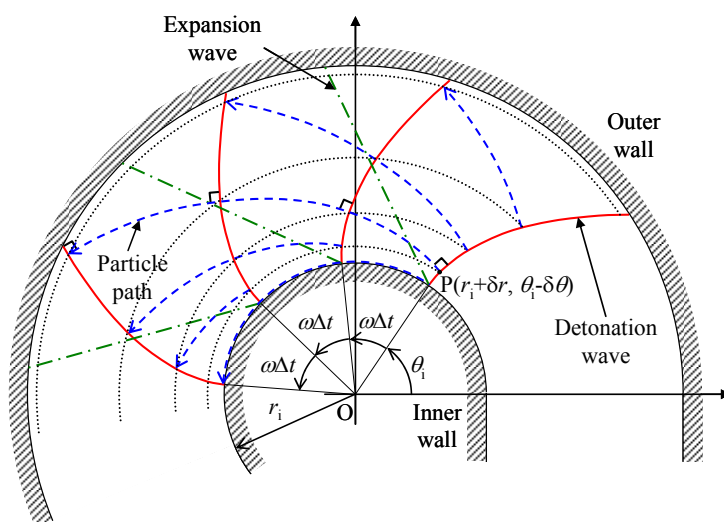
Fig. 11. Schematic of the behavior of the detonation wave in the stable propagation mode.
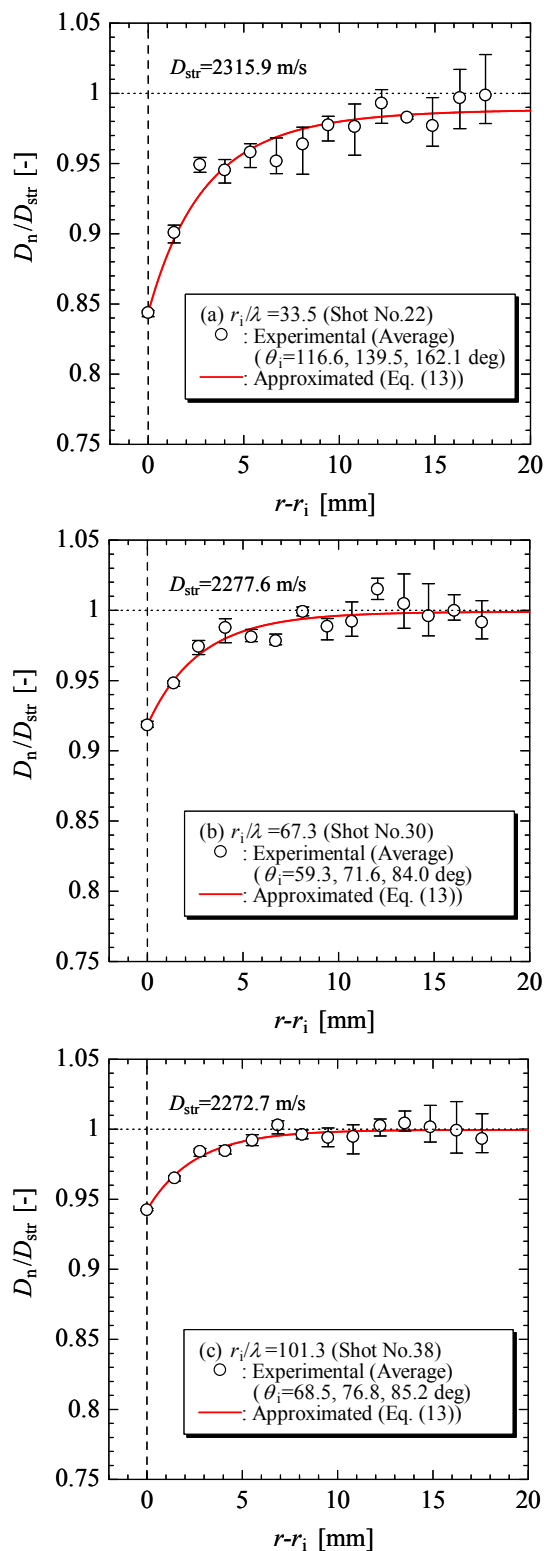
Fig. 12. Distribution of the normal detonation velocity on the detonation wave in the stable
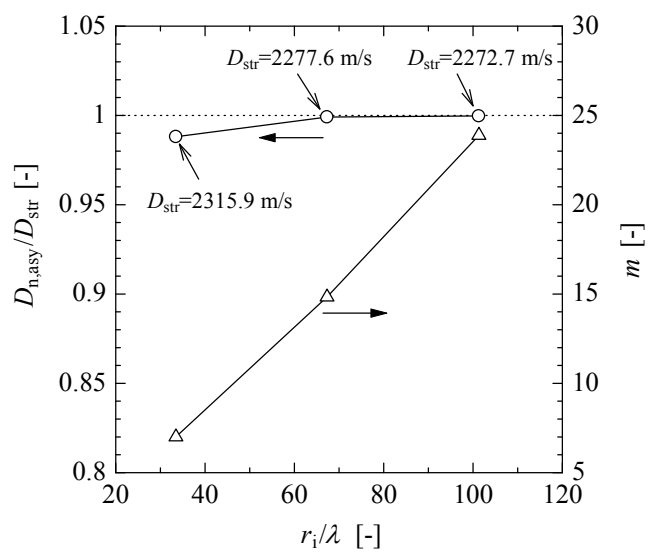
propagation mode.
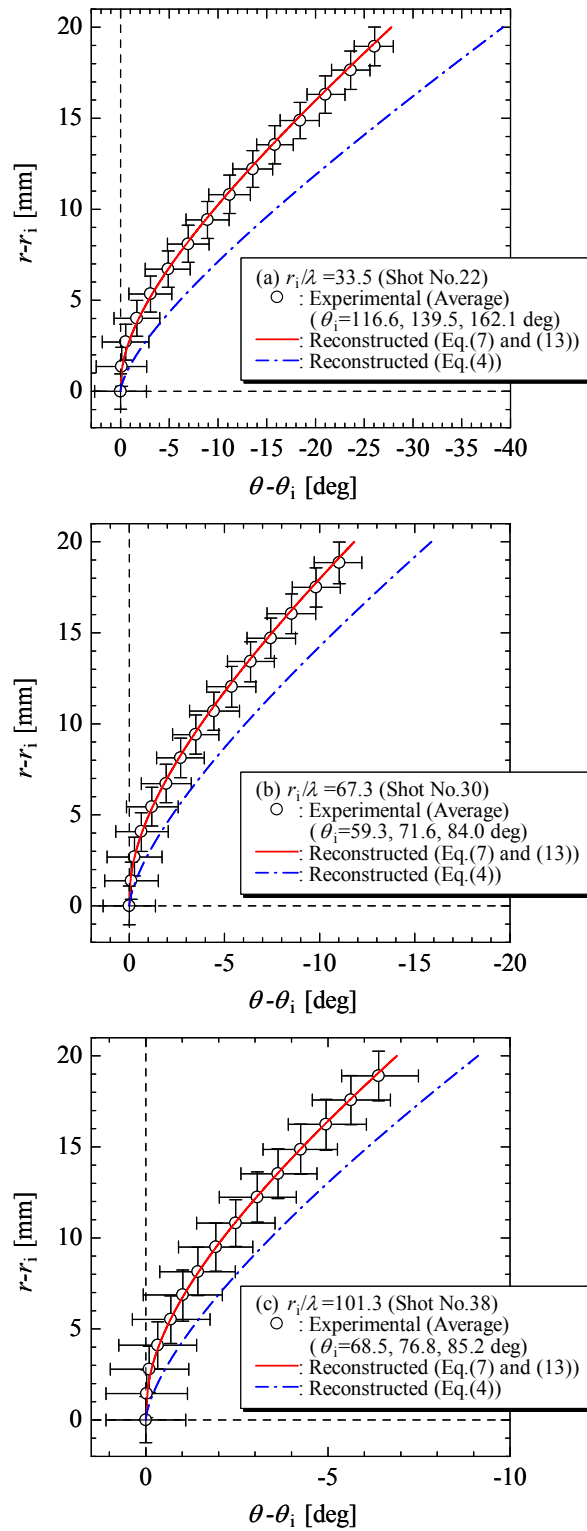
Fig. 13. Variations of $D_{n,asy}$ and m with r_i/λ.

Fig. 14. Front shock shape of the detonation wave in the stable propagation mode.
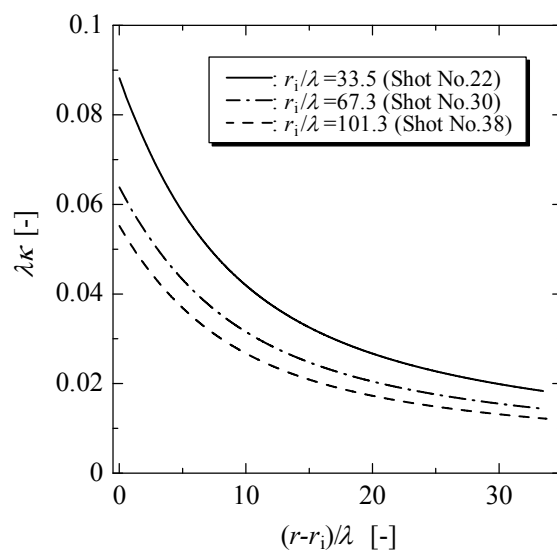
Fig. 15. Relation between $\lambda\kappa$ and $(r-r_i)/\lambda$ of the detonation wave in the stable propagation mode.
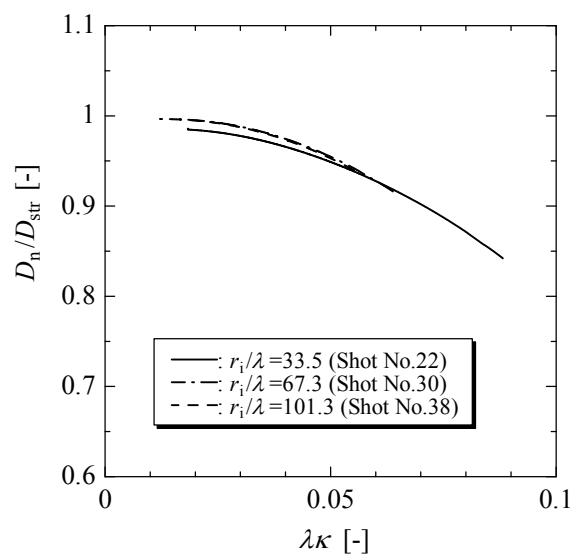
Fig. 16. Relation between D_n/D_{str} and $\lambda\kappa$ of the detonation wave in the stable propagation mode.